Journal of Electroanalytical Chemistry 931 (2023) 117214

Contents lists available at ScienceDirect

Journal of Electroanalytical Chemistry

journal homepage: www.elsevier.com/locate/jelechem

Evaluation of mass transfer behaviour of sulfamethoxazole species at ion–exchange membranes by chronopotentiometry for electrodialytic processes

Kayo Santana Barros [a,b,c,*], Alexandre Giacobbo [a], Gustavo Dall Agnol [a], Svetlozar Velizarov [b], Valentín Pérez–Herranz [c], Andréa Moura Bernardes [a]

[a] Post-Graduation Program in Mining, Metallurgical and Materials Engineering (PPGE3M), Federal University of Rio Grande do Sul (UFRGS), Av. Bento Gonçalves, 9500, Porto Alegre 91501-970, Brazil

[b] Associated Laboratory for Green Chemistry-Clean Technologies and Processes (LAQV), REQUIMTE, Chemistry Department, FCT NOVA, Universidade Nova de Lisboa, Caparica 2829-516, Portugal

[c] IEC Group, ISIRYM, Universitat Politècnica de València, Camí de Vera s/n, 46022, P.O. Box 22012, València E-46071, Spain

ARTICLE INFO

Keywords:
Organic micropollutants
Sulfamethoxazole
Sorption
Electrodialysis
Chronopotentiometry

ABSTRACT

In recent years, electrodialysis has been often considered as an appropriate method to treat industrial and/or municipal wastewater containing pharmaceutically active compounds. However, the scarcity of information on the ion transport mechanisms through the membranes, especially concerning occurrence of possible sorption phenomena, has limited the process implementation in practice. The present work aims to evaluate, by chronopotentiometry, the transport of sulfamethoxazole (SMX) through a cation- (CEM) and anion-exchange membrane (AEM) using synthetic solutions at different concentrations (0.001–0.1 g/L) and pH conditions (1.6 for CEM and 9 for AEM). The dominant mechanism of mass transfer under overlimiting current conditions at each membrane/solution system was determined. The potential drop profile measured during and after application of current pulses, as well as the transition times obtained from the curves, showed that sorption occurs at/in both membranes, especially for the AEM. Besides, this phenomenon was reversible for the CEM and irreversible for the AEM under the conditions evaluated herein. The chronopotentiograms of the AEM showed that the intense occurrence of water dissociation with the most diluted solution caused chemical equilibrium shifts in the membrane/electrolyte system, leading to formation of neutral SMX species that can impair the electrodialysis performance. The results obtained are useful for optimizing the electrodialytic treatment of SMX-containing solutions as well as of other compounds with similar physicochemical properties.

1. Introduction

The presence of organic micropollutants (OMPs) in the environment, both generated in industries and released from humans and animals, has caused serious concerns, because these contaminants can compromise the human health and aquatic ecosystems at concentrations in the order of μg/L – ng/L [1]. OMPs are frequently found in different aquatic systems, such as surface water, groundwater, drinking water, municipal and industrial wastewater [2]. The presence of antibiotics in water bodies has been of particular concern due to increasing antibiotic resistance of commensal and pathogenic bacteria [3]. This antibiotic resistance dissemination occurs mainly due to their presence in municipal sewage collectors and treatment plants of wastewater, especially those from hospitals [4]. Among the antibiotics responsible for this situation, sulfamethoxazole (SMX) requires a special attention, since it is one of the most used antibiotics for treating urinary tract infections in humans and animals, in addition to digestive and bronchopulmonary infections [5,6]. The presence of SMX in aqueous effluents is of great concern as it is hardly degraded via biological routes, making it highly persistent [7]. Overcoming this situation is challenging since the conventional systems used in the treatment of such effluents are not specifically designed to deal with this type of contaminants. Therefore, in recent years, researchers have evaluated the use of alternative methods for removing pharmaceutically active

* Corresponding author at: Post-Graduation Program in Mining, Metallurgical and Materials Engineering (PPGE3M), Federal University of Rio Grande do Sul (UFRGS), Av. Bento Gonçalves, 9500, Porto Alegre 91501-970, Brazil.
E-mail address: kayo.barros@fct.unl.pt (K.S. Barros).

https://doi.org/10.1016/j.jelechem.2023.117214
Received 21 November 2022; Received in revised form 18 January 2023; Accepted 29 January 2023
Available online 1 February 2023

compounds (PhACs) from industrial and municipal wastewater streams using membranes, such as membrane bioreactor [2], ultrafiltration [8], nanofiltration [9], reverse osmosis [10] and electrodialysis [11–13].

Electrodialysis is a highly versatile electro-driven membrane separation process which has been considered in several applications [14,15]. The use of electrodialysis to treat municipal wastewater has stood out, as it allows the recovery of valuable macronutrients, such as phosphorus, nitrogen and potassium, in addition to the removal of various micropollutants, including PhACs [16,17]. Compared with pressure–driven membrane separation processes, electrodialysis is advantageous because it allows frequent electrode polarity reversal, which mitigates membrane fouling/scaling [11,15,18]. In the case of treatments of PhACs–containing solutions by electrodialysis, which can be present as cations, anions or neutral species depending on the pH, the physicochemical properties of the target species (i.e. charge, size, and hydrophobicity) have been shown to influence significantly their transport through the membranes [8,12,13,19,20]. However, information on the transport mechanisms of these species through ion-exchange membranes are still scarce in the literature.

In recent years, one of the most studied issues involving the treatment of antibiotics–containing aqueous streams by electrodialysis has been the effect of their sorption at/in the membranes on their separation performance [12,13,21]. Roman et al. [13] evaluated the transport of 19 OMPs through commercial anion- (AEM) and cation–exchange membranes (CEM) and verified that 1) positively charged OMPs were strongly adsorbed inside the membrane and weakly transported across it, 2) negatively charged OMPs were weakly adsorbed at the membrane surface but transported extensively across it, and 3) non-charged OMPs were hardly adsorbed inside the membrane or at its surface, but were transported through it by diffusion. On the other hand, Ma et al. [22] recently evaluated the transfer of 25 OMPs present in real wastewaters through cation- and anion-exchange membranes and noted that negatively charged OMPs undergo a stronger decrease in their rate of transport across anion-exchange membranes due to sorption effects compared to non– and positively charged OMPs. Thus, to ensure that electrodialysis is a feasible technique for treating solutions containing organic micropollutants, it is necessary to carry out dedicated studies on the transport of the target organic micropollutants across the membranes. In general, these studies are conducted in electrodialytic systems by evaluating the percentage of chemical species that cross the membrane. In this sense, the adsorbed chemical species are accounted for by closing the respective mass balances in the feed and receiver compartments [16,21,22]. Although these studies are essential to evaluate the extent of adsorption at/in the membranes used, they do not allow for a critical assessment of the reasons for the sorption occurrence and the mechanisms responsible for this phenomenon. For this, dynamic characterization methods must be used, such as impedance spectroscopy [23,24], linear sweep voltammetry [25,26] and chronopotentiometry [27,28]. Among the aforementioned techniques, the use of chronopotentiometry stands out because it allows for a direct access to the electric potential contribution in different states of the membrane/electrolyte system [29].

Chronopotentiometry is an electrochemical technique that allows for the determination of the membrane potential drop during and after the application of an electric current pulse. The curves obtained, referred to as chronopotentiograms, provide important information on the membrane/solution system, such as the time taken for the concentration polarization occurrence (transition time), in addition to allow for determining the dominant mass transfer mechanism, such as diffusion/migration, electroconvection, gravitational convection, and water dissociation at different operating conditions. From the values of membrane potential drop obtained by chronopotentiometry, current–voltage curves (or polarization curves) can be constructed, which also provide useful information such as the limiting current density, ohmic resistance, and the energy involved in the alteration of the dominant mechanism of ion transfer when concentration polarization takes place, which is called plateau length. In addition, both chronopotentiometric and current–voltage curves provide information regarding competition between species to migrate across the membranes [27,30] and occurrence of fouling/scaling [31]. Although chronopotentiometry is highly valuable for evaluating membrane systems, to the best of our knowledge, there is no work in the open literature on the use of this technique to evaluate the mass transfer mechanisms and the effect of sorption at ion-exchange membranes in electrodialytic treatments of SMX-containing solutions.

Therefore, the present work aims to evaluate, by chronopotentiometry, the properties and mechanisms of ion transport through membranes present in electrodialysis systems applied to treat water and wastewater containing SMX. Chronopotentiometric and current–voltage curves were obtained for an anion- and cation–exchange membrane with synthetic solutions at four concentration conditions (0.001 g/L; 0.005 g/L; 0.01 g/L; 0.1 g/L) based on the chemical composition of municipal and pharmaceutical wastewaters [6,32,33]. Two pH values were evaluated (1.6 for the CEM and 9 for the AEM), which were chosen based on speciation diagrams constructed herein. Limiting current densities, ohmic resistances, plateau lengths and transition times were determined from the curves. The occurrence of sorption and mass transfer phenomena at the membrane/solution interfaces under different operating conditions were evaluated from the curves obtained.

2. Materials and methods

2.1. Ion-exchange membranes

The membranes evaluated were the heterogeneous cation-exchange membrane IONSEP-HC-C (also known as HDX100) and the anion-exchange membrane IONSEP-HC-A (known as HDX200) manufactured by Hangzhou Iontech Environmental Technology Co. (China). In the evaluation of each membrane, the other was also present in the system to reduce the possible effect of reactions occurring at the electrodes. Both membranes have been frequently used in electrodialysis and chronopotentiometry studies [27,34,35], and their main characteristics can be found elsewhere [36].

2.2. Working solutions

Chronopotentiometric and current–voltage curves were obtained for the cation- and anion–exchange membranes using synthetic solutions at four SMX concentrations (0.001 g/L; 0.005 g/L; 0.01 g/L; 0.1 g/L) at pH 1.6 for the evaluation of the CEM and pH 9 for the AEM. The solutions were freshly prepared with SMX, having a purity greater than 99 % and purchased in a pharmacy (Porto Alegre, Brazil), and distilled water. The solution pH was adjusted with H_2SO_4 and NaOH (Química Moderna Ind. e Com. Ltda, Barueri, Brazil). The concentration values tested were based on the composition of SMX in municipal and pharmaceutical wastewaters [6,32,33], whereas the pH values were based on the speciation diagram presented in Section 3.

2.3. Chronopotentiometric experiments

The chronopotentiometric experiments were performed in an electrochemical cell containing three compartments separated by an anion- and cation-exchange membrane (Fig. S1 of Supplementary Material). Two graphite electrodes placed at the ends of the cell were used as working and counter-electrodes. The electric current was supplied by a potentiostat/galvanostat (Autolab, PGSTAT30, Utrecht, The Netherlands). The potential drop of the evaluated membranes under

the application of a current pulse was measured using Ag/AgCl electrodes, which were immersed in Luggin capillaries and positioned at the two opposite membrane surfaces facing its cathodic and anodic sides. The effective area of the membranes was 3.14 cm^2 and before the tests they were maintained for 24 h in the solution to be evaluated. The experiments were conducted at room temperature (~20 °C) and with no stirring. The tests were performed in duplicate and the calculated relative error between the obtained data was lower than 6 %. The chronopotentiometric curves were recorded by applying current for 400 s. After 400 s, the current application was interrupted to allow for relaxation of the membrane system for 100 s so that the next current pulse could be applied. The current–voltage curves of the membrane/solution systems were constructed using the values of each applied current density and the potential drop measured immediately before the relaxation step.

2.4. Determination of the transport properties of the membrane/solution systems

Fig. S2 of Supplementary Material presents a representation of a typical current–voltage curve showing three distinct regions, which provides the transport properties evaluated herein. The limiting current density (i_{lim}) was obtained by determining the intersection point of the tangential lines of the ohmic region (region I) and the plateau region (region II). The ohmic resistance (R_{ohm}) was estimated by the inverse of the slope (α) of the tangential line of the ohmic region. The plateau length was estimated by subtracting the final and initial potential drop values of region II.

Transition times (τ) were obtained for each applied current pulse under overlimiting regime from the maximum point (inflection point) of the derivative of the membrane potential drop with respect to time, as shown in Fig. S3 of Supplementary Material.

3. Results and discussion

In order to evaluate the influence of concentration and pH of the solutions on ion transfer through the cation- and anion- membranes, speciation diagrams for SMX at 0.001 g/L, 0.005 g/L, 0.01 g/L and 0.1 g/L were constructed with the aid of Chemicalize software, as shown in Fig. 1. The predominant species in a wide pH range is neutral, which would make the use of electrodialysis at this condition unfeasible. Thus, two pH values at which ionic species are predominant were evaluated: 1.6 and 9. As at pH 1.6 the predominant SMX species is a cation (SMX-H_3N^+), the membrane evaluated at this condition was the cation–exchange one. On the other hand, the membrane evaluated at pH 9 was the anion–exchange one since the predominant SMX species is an anion (SMX–N^-). Note that at pH 1.6, the concentration of protons is considerably higher than the concentration of SMX species in the solutions at 0.001 g/L, 0.005 g/L and 0.01 g/L, whereas the concentration of protons and SMX-H_3N^+ are identical in the solution at 0.1 g/L and pH 1.6. Concerning the solutions at pH 9 used for evaluating the AEM, the predominant species for all SMX concentrations is SMX-N^-, showing a large concentration difference between these ions and OH^-, especially in the most concentrated solutions.

3.1. Evaluation of the cation-exchange membrane

3.1.1. Chronopotentiometric curves for the CEM

The chronopotentiometric curves obtained for the cation-exchange membrane with SMX solutions at 0.001 g/L, 0.005 g/L, 0.01 g/L and 0.1 g/L and pH 1.6 are shown in Fig. 2.

The chronopotentiometric curves of the cation-exchange membrane showed different shapes in function of the SMX concentration. For all tested solutions, the curves obtained under low current densities (see 3.2 mA/cm^2 in Fig. 2(a – d)) showed a linear behavior over time, indicating that ion transport through the membrane is governed by diffusion–migration. As the intensity of the current density increased, the curves began to show the typical inflection point related to the occurrence of intense concentration polarization, and at current densities greater than the i_{lim} overlimiting mechanisms such as electroconvection and water dissociation were activated.

The curves of the solution at the lowest SMX concentration (0.001 g/L – Fig. 2(a)) showed the occurrence of intense electroconvection under high current densities, indicating that this mechanism is predominant over the others in the overlimiting regime. The intense oscillations of the potential drop at current densities of 11.1 mA/cm^2 and 12.7 mA/cm^2 indicate that the dominant electroconvection type in this membrane/solution system is the unstable one, also known as Rubinstein-Zaltzman electroconvection mode [38]. This type of electroconvection suppresses the occurrence of other overlimiting mechanisms such as water dissociation due to the large vortices formed at the membrane surface [39]. Indeed, the curves do not suggest the occurrence of water dissociation or gravitational convection. Among the solutions evaluated, the electroconvection occurred with greater intensity with the most diluted one due to the thicker space charge region near the membrane surface [38].

The curves obtained for the solution at concentration of 0.005 g/L (Fig. 2(b)) showed similar behaviors to the curves of the solution at 0.001 g/L. Note that under high current densities (15.9 mA/cm^2 and 19.1 mA/cm^2), electroconvection occurred intensely at the membrane surface, as oscillations in the potential drop were observed. However, the curves indicate that water dissociation occurred simultaneously with electroconvection, as the curves showed a subtle reduction in potential drop after reaching a maximum point, as indicated in Fig. 2(b). The water dissociation phenomenon occurs in a thin layer at the membrane/solution interface as proton-transfer reactions involving water molecules and the membrane fixed charged groups [40,41]. Thus, the membrane type and electrolyte condition influence strongly this phenomenon. When water dissociation occurs, H^+ and OH^- ions are generated, altering considerably the pH inside the membrane as the counter-ions are transferred through it and at its surface due to the Donnan exclusion of co-ions. Thus, the reduction in potential drop shown in Fig. 2(b) can be explained by the water dissociation occurrence and the consequent formation of the conductive H^+ and OH^- ions. In this sense, H^+ ions were transported intensively through the CEM, while OH^- ions were retained at its surface, thus reducing the resistance of the membrane/solution system [42]. As electroconvection and water dissociation occurred simultaneously with the 0.005 g/L solution, neither phenomenon was able to completely suppress the other, indicating that they are competitive at this SMX concentration.

For the solution at 0.01 g/L, the curves under high current densities (15.9 mA/cm^2 and 17.5 mA/cm^2 – Fig. 2(c)) showed subtle oscillations in the potential drop, less intense than those verified for the more diluted solutions, which indicates that electroconvection does not occur strongly in this membrane/solution system. On the other hand, water dissociation occurred intensely, as a maximum point was observed in the curves followed by a reduction in the potential drop associated with the formation of H^+ and OH^- ions. This indicates that increasing the concentration of SMX from 0.001 g/L to 0.01 g/L, the dominant overlimiting mechanism is altered from electroconvection to water dissociation. In general, the occurrence of water dissociation is undesirable in electrodialysis systems because it increases the energy consumption, which is not associated with an increase in the target ion(s) transport [29]. Besides, it might favor the occurrence of fouling/scaling.

The curves obtained for the 0.1 g/L solution did not suggest the occurrence of intense electroconvection, while the potential drop measured for high current densities showed a subtle peak followed by its reduction over time (28.7 mA/cm^2 and 31.8 mA/cm^2 – Fig. 2(d)). This subtle peak could be associated with the occurrence of water

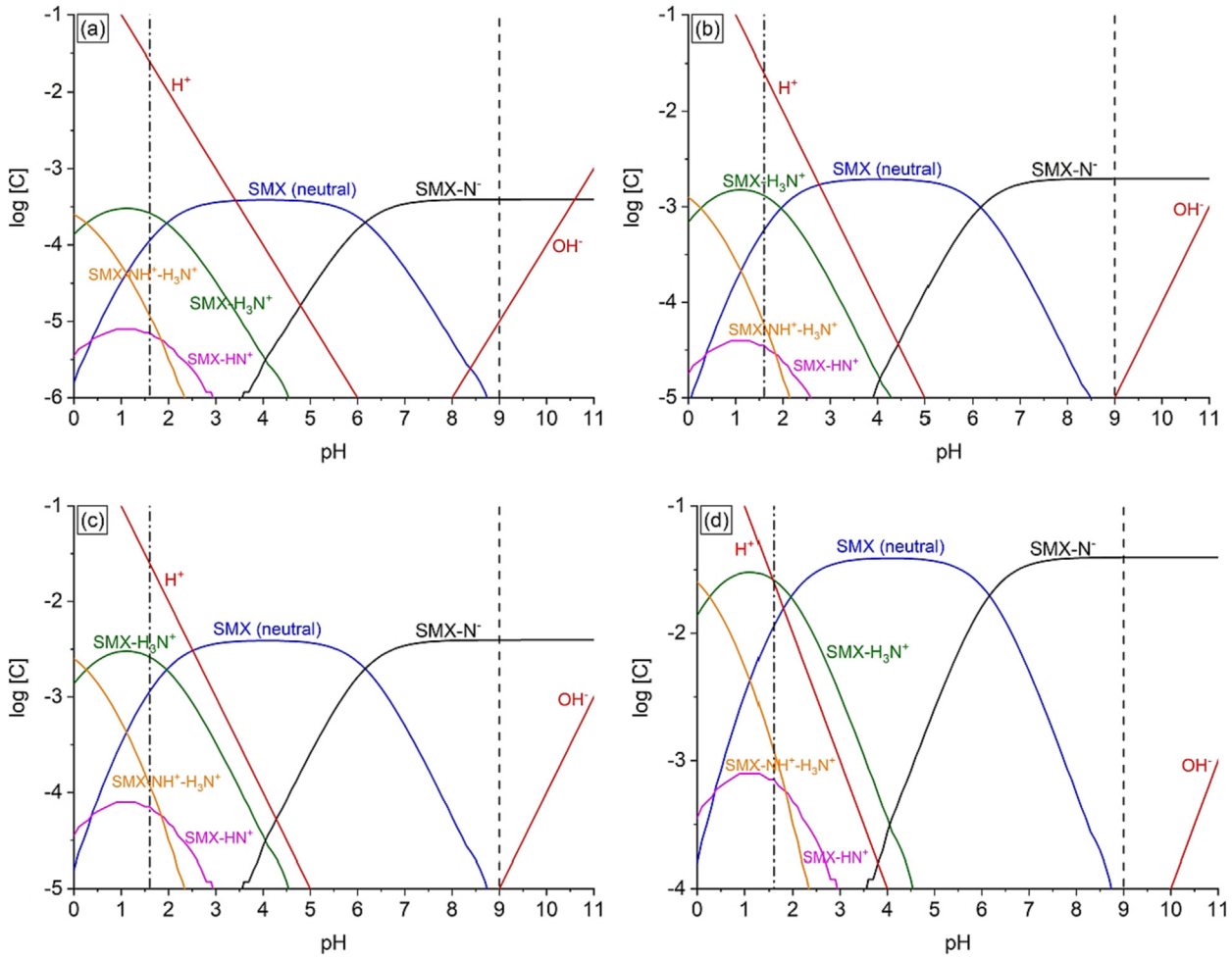

Fig. 1. Speciation diagrams for the solutions at SMX concentrations of (a) 0.001 g/L, (b) 0.005 g/L, (c) 0.01 g/L and (d) 0.1 g/L constructed with the aid of Chemicalize software [37]. The dashed lines indicate pH 1.6 and pH 9.

dissociation, as verified for the 0.005 g/L and 0.01 g/L solutions, and/or the emergence of gravitational convection, which also causes the appearance of a maximum point on a chronopotentiogram [43,44]. However, gravitational convection is relevant only when the electrolyte concentration is greater than approximately 5×10^{-2} mol/L (For a NaCl solution) [45,46], which is a value considerably higher than the molar concentration of SMX at the 0.1 g/L solution (3.95×10^{-4} mol/L). Thus, it is most likely that the dominant mechanism responsible for the reduction in potential drop over time with the solution at 0.1 g/L is water dissociation.

It is worth noting that the values of potential drop recorded immediately after imposition of each current pulse increased as the solution concentration increased. This initial potential drop is related to the ohmic potential drop (E_Ω – indicated in Fig. 2(a)) over the membrane and the two adjacent solutions when the membrane/solution system is not yet under the effect of concentration polarization [47]. The increase of E_Ω with increasing solution concentration (compare Fig. 2(a – d)) indicates that the presence of SMX increases the resistance of the non–polarized liquid diffusion boundary layer, and this may be related to the well-known sorption effect of this component at/in the membrane. This phenomenon has been frequently evaluated in the literature as it affects considerably the performance of membrane processes to treat PhACs-containing water/wastewater [8,21,48]. In electrodialysis systems, the sorption effect depends on several factors, such as solute properties (charge, polarity, size, and hydrophobicity), membrane structure properties (morphology), electrostatic interactions between the target pharmaceutical compounds and the membrane, in addition to the level of applied current density (underlimiting or overlimiting current regime) [12,13,16,21]. The curves shown in Fig. 2 indicate that the intensity of sorption phenomenon increases considerably with increasing the SMX concentration. As SMX is generally present in municipal wastewater in concentrations on the order of μg/L – ng/L [1], the sorption effect of this component at/in the CEM on separationist transport should be insignificant. However, this may be of concern in the treatment of wastewater effluents originating from pharmaceutical industries, as the concentration of SMX in such effluents is usually on the order of mg/L [32,49] and can reach g/L [50].

After the interruption of the current density application, the potential dropped to a residual value very close to zero (E_c – shown in Fig. 2 (a)). This remaining potential difference across the membrane after switching-off the current represents the concentration overvoltage and appeared due to differences in the concentration profiles established at both surfaces of the membrane during current application [47]. Then, the potential drop related to the diffusion relaxation of the system approached zero over time, which is a typical behavior for monopolar membranes. This indicates that despite the occurrence of sorption at/in the CEM during the application of electric current, the membrane practically has returned to its initial condition after the application of each current pulse. Therefore, according to the

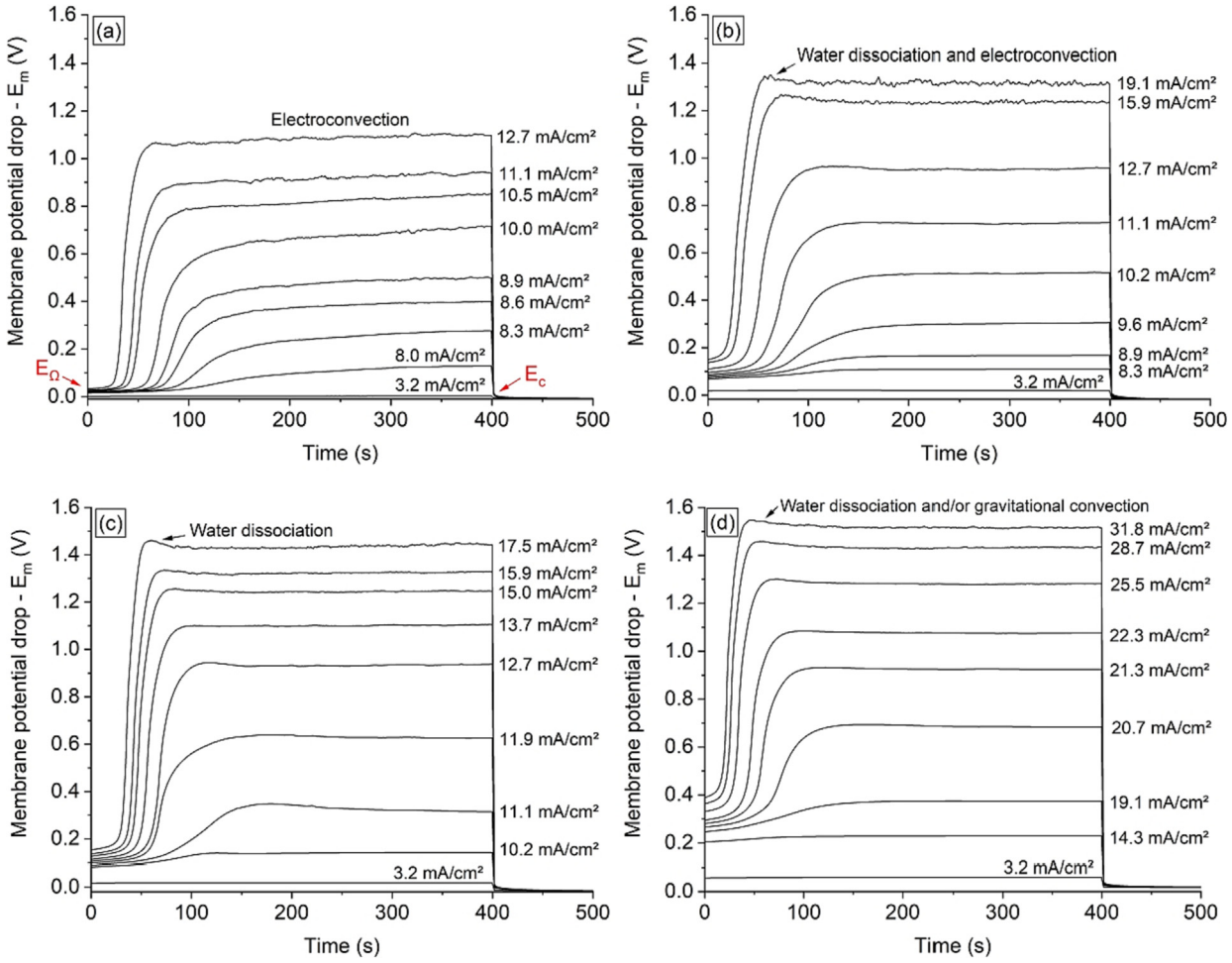

Fig. 2. Chronopotentiograms for the cation-exchange membrane with SMX solutions at pH 1.6 and concentration of (a) 0.001 g/L, (b) 0.005 g/L, (c) 0.01 g/L, and (d) 0.1 g/L.

chronopotentiograms, the sorption effect on the CEM shows to be relevant only during the application of electric current, which favors the electrodialysis operation since a post–treatment step to desorb the SMX is not required. This may be explained by the acidic solution pH and the ability of H^+ ions to desorb SMX ions, as verified for OH^- ions in alkaline medium [51].

Transition times were obtained for each current pulse under overlimiting regime from the maximum of the derivative of the membrane potential drop with respect to time. The transition time corresponds to the moment at which the depletion of ions takes place at the diffusion boundary layer because of intense concentration polarization occurrence [29]. This term is present in the well-known Sand Equation (Eq. (1)), where D is the electrolyte diffusion coefficient, C_0 is the bulk concentration, z_j is the charge of the counter-ion, $\bar{t}_j$ is the transport number of the counter–ion in the membrane phase, t_j is the transport number of the counter-ion in the solution, i is the current density and F is the Faraday's constant [27]. With the obtained τ values, curves showing the dependence of transition time on current density represented in Sand's coordinates were constructed, which are shown in Fig. 3. Only τ values obtained for current densities at least 1.5 times greater than the i_{lim} of the evaluated membrane system were considered for Sand Equation application, as indicated in the work of Mareev et al. [52].

$$\tau = \frac{\pi D}{4}\left(\frac{z_j F C_0}{\bar{t}_j - t_j}\right)^2 \left(\frac{1}{i^2}\right) \quad (1)$$

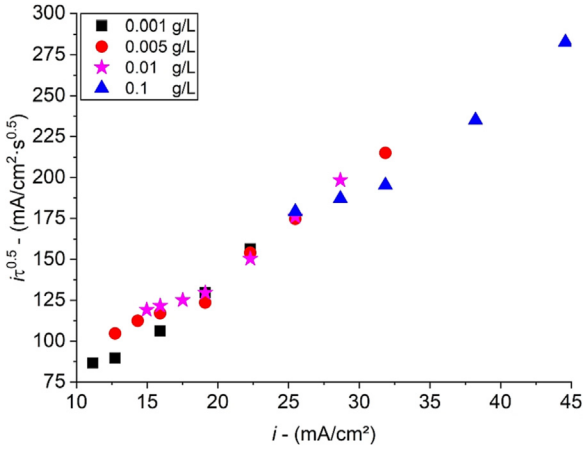

Fig. 3. Dependence of $i\tau^{0.5}$ on current density for the cation-exchange membrane with SMX solutions at pH 1.6 and concentrations of 0.001 g/L, 0.005 g/L, 0.01 g/L and 0.1 g/L.

Note that the points are virtually linear for all solutions tested, especially under the highest current densities, which indicates that the Sand equation can be applied for these membrane/solution systems [53]. On the other hand, the values of $i\tau^{0.5}$ varied in function of i without showing the typical horizontal behavior [31,54]. Note that

a positive and practically identical slope was verified for all SMX concentrations. In general, this dependence of $i\tau^{0.5}$ values in function of i is associated with the occurrence of chemical reactions in the membrane/electrolyte system simultaneously to ion transfer. In this sense, the intensity (subtle or strong) and type (negative or positive) of the plot slope determines the kinetics of the reactions [27,53]. In the case of the present study, the strong and positive slope of the curves shown in Fig. 3 should be associated with the occurrence of sorption of SMX simultaneously with its transfer across the membrane. The identical slope of the curves for all solutions supports this assumption since the membrane and ion type sorbed are the same. Therefore, the sorption kinetics is the same for all solutions tested.

3.1.2. Current-voltage curves for the CEM

The current–voltage curves constructed for the cation-exchange membrane with solutions at pH 1.6 and concentrations of 0.001 g/L, 0.005 g/L, 0.01 g/L and 0.1 g/L are shown in Fig. 4. From the curves obtained, the limiting current density, ohmic resistance and plateau length of the membrane/solution systems were determined, which are shown in Table 1. The table also shows the cationic equivalent charge values (Q_{eq}^{+}), which were calculated by Eq. (2), where C_+ and z_+ are the concentration and charge of cationic species (obtained from Fig. 1).

$$Q_{eq}^{+} = \sum z_+ C_+ \quad (2)$$

The curves obtained for the four solutions showed three well-defined regions, which is a typical shape for monopolar membranes. The limiting current density showed a linear behavior as a function of Q_{eq}^{+} for the 0.001 g/L, 0.005 g/L and 0.01 g/L solutions (Fig. S4 (a) of Supplementary Material), as expected [28,55]. However, the relationship between Q_{eq}^{+} and i_{lim} deviated from linearity considering the solution at 0.1 g/L, since the i_{lim} obtained was lower than the expected one. This can be explained by the sorption phenomenon occurring more intensely with the more concentrated solution, and the consequent reduction of the fraction of membrane conductive area due to its clogging. According to the modified Sand Equation, which presents the fraction of membrane conductive area term, the lower the fraction of conductive area, the lower the i_{lim} [56]. The ohmic resistance showed an opposite behavior to the expected one, since R_{ohm} increased with the increase of Q_{eq}^{+} [27,30]. This can also be explained by the sorption of SMX and the consequent clogging of the membrane. In this sense, the effective membrane area available for ion exchange is reduced, thus reducing the available ion-exchange capacity provided by the fixed functional groups leading to increasing membrane resistance [22]. According to Table 1, the plateau length increased with increasing SMX concentration. The plateau of the current–voltage curve is a transition region between the ohmic region and the overlimiting region of the curve (see Fig. S2). Therefore, the plateau length is a representation of the energy involved in the disruption event of the diffusion boundary layer leading to alteration in the dominant ion transfer mechanism from migration-diffusion to overlimiting phenomena. In this sense, the shorter plateau length for the most diluted solutions means that the electroconvection occurrence is favored with these solutions, which is in line with the discussion presented for the chronopotentiograms. This favors the treatment of water streams contaminated with SMX by electrodialysis since Welter et al. [21] recently found that the transport of PhACs by cation-exchange membranes is significantly enhanced at overlimiting current regime. In addition, Pronk et al. [57] verified that the intensity of sorption occurrence in an electrodialysis system was very high initially, but considerable breakthroughs occurred during extended operation, which should also be related to the dominance of overlimiting mechanisms over operation time. Therefore, the lower the concentration, the more intense the electroconvection, which enhances the SMX transfer through the membrane.

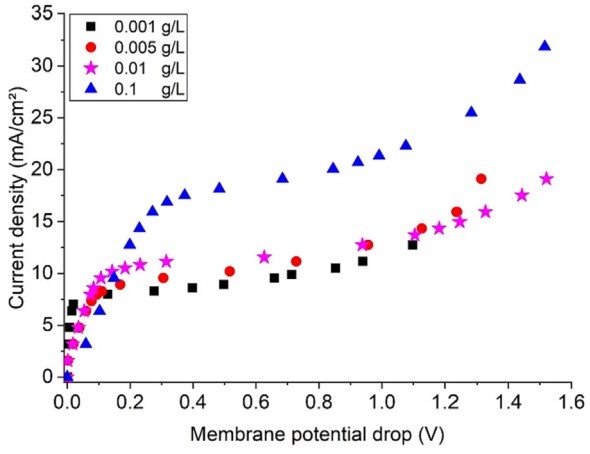

Fig. 4. Current-voltage curves for the cation-exchange membrane with SMX solutions at pH 1.6 and concentrations of 0.001 g/L, 0.005 g/L, 0.01 g/L, and 0.1 g/L.

Table 1
Cationic equivalent charge (Q_{eq}^{+}), limiting current density (i_{lim}), ohmic resistance (R_{ohm}) and plateau length values obtained for the cation-exchange membrane with solutions at pH 1.6 and SMX concentrations of 0.001 g/L, 0.005 g/L, 0.01 g/L and 0.1 g/L.

SMX concentration (g/L)	0.001	0.005	0.01	0.1
Q_{eq}^{+}(meq/L)	254.1	265.8	280.4	543.8
i_{lim} (mA/cm^2)	7.69	8.6	10.41	16.95
R_{ohm} (Ω.cm^2)	3.3	10.3	10.1	15.3
Plateau length (V)	0.63	0.79	1.05	1.04

The curves obtained for the four solutions showed three well-defined regions, which is a typical shape for monopolar membranes. The limiting current density showed a linear behavior as a function of Q_{eq}^{+} for the 0.001 g/L, 0.005 g/L and 0.01 g/L solutions (Fig. S4 (a) of Supplementary Material), as expected [28,55]. However, the relationship between Q_{eq}^{+} and i_{lim} deviated from linearity considering the solution at 0.1 g/L, since the i_{lim} obtained was lower than the expected one. This can be explained by the sorption phenomenon occurring more intensely with the more concentrated solution, and the consequent reduction of the fraction of membrane conductive area due to its clogging. According to the modified Sand Equation, which presents the fraction of membrane conductive area term, the lower the fraction of conductive area, the lower the i_{lim} [56]. The ohmic resistance showed an opposite behavior to the expected one, since R_{ohm} increased with the increase of Q_{eq}^{+} [27,30]. This can also be explained by the sorption of SMX and the consequent clogging of the membrane. In this sense, the effective membrane area available for ion exchange is reduced, thus reducing the available ion-exchange capacity provided by the fixed functional groups leading to increasing membrane resistance [22]. According to Table 1, the plateau length increased with increasing SMX concentration. The plateau of the current–voltage curve is a transition region between the ohmic region and the overlimiting region of the curve (see Fig. S2). Therefore, the plateau length is a representation of the energy involved in the disruption event of the diffusion boundary layer leading to alteration in the dominant ion transfer mechanism from migration-diffusion to overlimiting phenomena. In this sense, the shorter plateau length for the most diluted solutions means that the electroconvection occurrence is favored with these solutions, which is in line with the discussion presented for the chronopotentiograms. This favors the treatment of water streams contaminated with SMX by electrodialysis since Welter et al. [21] recently found that the transport of PhACs by cation-exchange membranes is significantly enhanced at overlimiting current regime. In addition, Pronk et al. [57] verified that the intensity of sorption occurrence in an electrodialysis system was very high initially, but considerable breakthroughs occurred during extended operation, which should also be related to the dominance of overlimiting mechanisms over operation time. Therefore, the lower the concentration, the more intense the electroconvection, which enhances the SMX transfer through the membrane.

On the other hand, the effect of overlimiting currents on the morphology of the membrane need to be evaluated, as they may cause erosions on the ion-exchange polymer that form cavities on the membrane surface [58].

3.2. Evaluation of the anion-exchange membrane

3.2.1. Chronopotentiometric curves for the AEM

The chronopotentiometric curves obtained for the anion-exchange membrane with solutions at pH 9 and concentrations of 0.001 g/L, 0.005 g/L, 0.01 g/L and 0.1 g/L are present in Fig. 5. Note that the curves show different behaviors from those obtained for the CEM.

The curves obtained for all solutions under low current densities showed the typical linear behavior over time, as expected, indicating that ion transport is governed by diffusion–migration at this condition (see 0.0010 mA/cm^2, 0.0032 mA/cm^2, 0.0064 mA/cm^2 and 0.0048 mA/cm^2 in Fig. 5(a – d), respectively).

For the 0.001 g/L solution (Fig. 5(a)), the curves showed the typical inflection point related to the occurrence of intense concentration polarization as the current density was increased (see the curve at 0.0096 mA/cm^2). In this case, the potential drop increase due to concentration polarization appeared immediately after the imposition of electric current without showing an almost linear region before the rapid increase, which usually appears in chronopotentiograms due to the development of small concentration gradients in the solution near the membrane surface (as verified for the CEM curves in approximately 0–50 s – Fig. 2) [29]. This increase in potential drop immediately after imposition of the current pulses verified for the AEM indicates that when overlimiting current densities are applied, the overlimiting phenomena at the membrane are activated very quickly, preventing ion transport across the membrane from being initially gov-

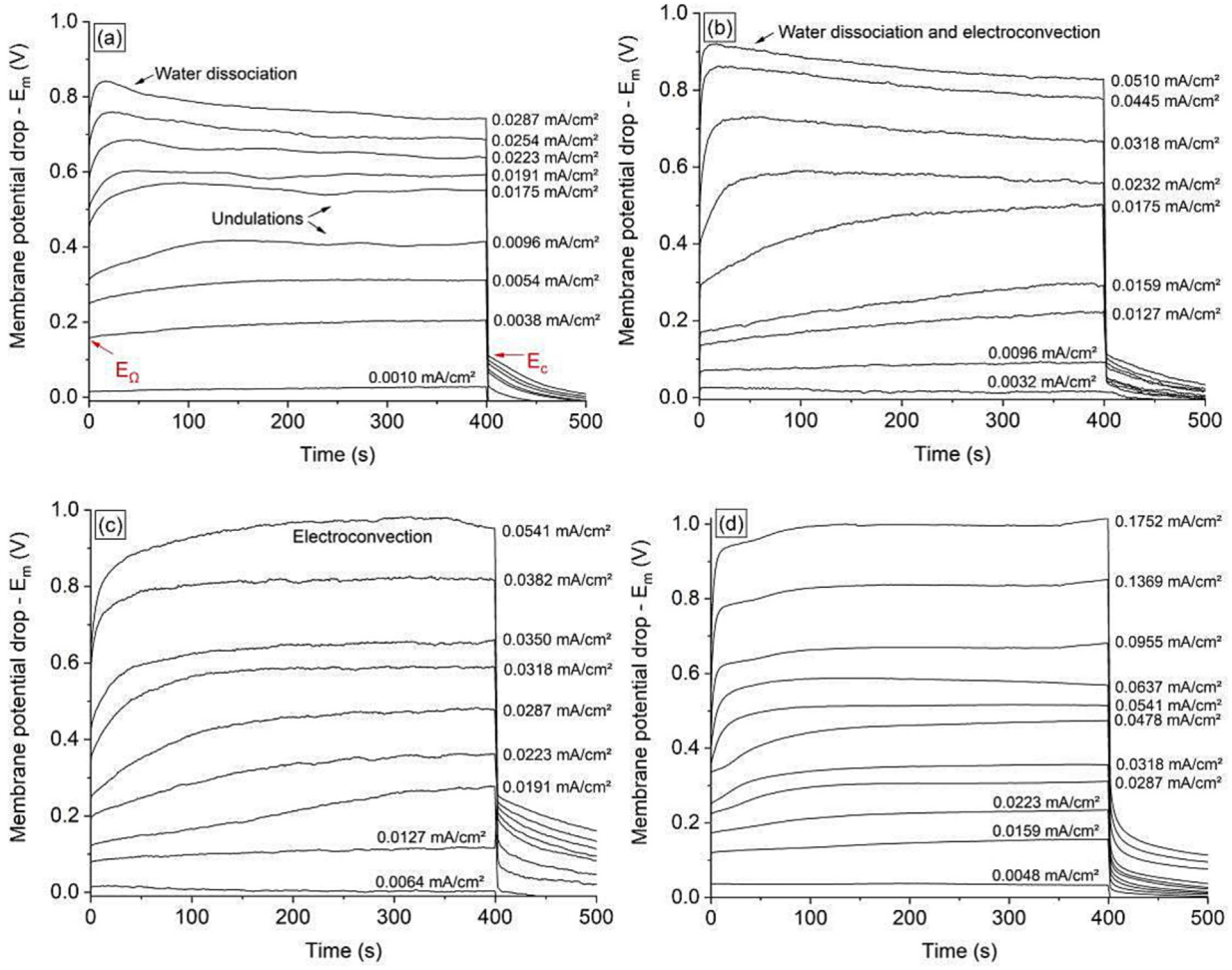

Fig. 5. Chronopotentiograms for the anion-exchange membrane with SMX solutions at pH 9 and concentrations of (a) 0.001 g/L, (b) 0.005 g/L, (c) 0.01 g/L, and (d) 0.1 g/L.

erned by electro–diffusion mechanisms [44]. Unlike the curves shown for the cation-exchange membrane at 0.001 g/L, the ones obtained for the AEM at this concentration under the highest current densities do not suggest the occurrence of intense electroconvection since the potential drop did not show typical oscillations related to vortexes formation at the membrane surface. On the other hand, the curves indicate a strong occurrence of water dissociation since the potential drop showed a peak after its rapid increase followed by an intense reduction over time, which occurred due to the formation of the conductive H^+ and OH^- ions at the membrane surface. This difference in the predominant overlimiting mechanism at each membrane is in agreement with the literature, since water dissociation tends to occur more intensely at AEMs than CEMs due to the greater catalytic activity of the functional groups of the former (quaternary ammonium groups) than the latter (sulfonic acid groups) towards this kind of reaction [59]. Besides, the occurrence of water dissociation at AEMs leads to the conversion of quaternary ammonium groups into tertiary amines, which have an even higher catalytic activity towards water dissociation reaction [60]. It can also be noticed that the potential drop showed some undulations (indicated in Fig. 5(a)) over time with successive increases and decreases especially at moderate current densities (0.0096 mA/cm^2 – 0.0223 mA/cm^2). Note that this only occurred with the most diluted solution, indicating that the undulations may be related to the greater proximity of the concentrations of the predominant SMX species (SMX-N^-) and OH^- ions (Fig. 1), in addition to the intense occurrence of water dissociation with this solution. In this case, the simultaneous transfer of SMX–N^- and OH^- ions and the consequent change in pH inside the membrane and at its surface is expected to have caused a shift in the chemical equilibrium of the SMX species being transferred through the membrane. It is well known that as OH^- ions are transferred intensively through an anion-exchange membrane, the pH inside it increases, while the pH at its surface decreases due to the Donnan exclusion of H^+ ions [27,61]. This phenomenon may have led to changes in the species present predominantly in the membrane/solution system, influencing the species transferred through the membrane – note in Fig. 1 that a reduction in pH at the membrane surface would lead to the formation of the neutral SMX species. The formation of this neutral species may impair the separation of SMX by electrodialysis since the absence of charges hinders its transfer through the membrane. The lower the concentration of SMX in solution, the greater the intensity of water dissociation and formation of neutral SMX species since the magnitude of Donnan co–ions (protons in this case) exclusion is enhanced with the external electrolyte solution dilution.

The curves obtained with the 0.005 g/L solution showed similar shapes to those shown for the 0.001 g/L solution. The potential drop presented a strong reduction after reaching a maximum point under overlimiting current densities (0.0510 mA/cm^2), which indicates intense water dissociation occurrence. In this case, the potential drop undulations related to equilibrium shifts shown for the 0.001 g/L solution were not verified, which can be explained by the higher distance between the concentration of SMX-N^- and OH^- species in this solution

(Fig. 1). The curves also showed typical oscillations related to electroconvection. Although electroconvection and water dissociation are competitive mechanisms [38,62], they occurred simultaneously at the membrane with the solution at 0.005 g/L, as verified for the cation-exchange membrane.

The behavior of the curves obtained for the solutions at 0.01 g/L and 0.1 g/L during concentration polarization is quite similar to the previous solutions: the potential drop increases rapidly without showing an almost linear region before the increase, indicating that concentration polarization occurs very quickly at the AEM. On the other hand, regarding the overlimiting ion transfer mechanisms, the curves obtained for both solutions did not show a maximum peak of potential drop followed by its reduction, indicating that, unlike the 0.001 g/L and 0.005 g/L solutions, water dissociation does not occur intensively in these systems. The curves for the 0.01 g/L solution showed the typical oscillations of electroconvection, whereas the curves for the 0.1 g/L solution did not suggest the occurrence of this phenomenon. Therefore, for the AEM with the most concentrated solution, no overlimiting mechanism of mass transfer plays a dominant role.

For all solutions tested, a significant increase in the ohmic potential drop (E_Ω – indicated in Fig. 5(a)) was observed as the current density increased. As discussed for the CEM in Section 3.1.1., this increase in E_Ω indicates that the presence of SMX increases the resistance of the non-polarized liquid diffusion boundary layer, which must be related to the sorption effect of this component at/in the membrane. Dedicated studies must be conducted to investigate in detail the distinct resistances of the membrane/electrolyte systems evaluated herein and their relationship with the sorption occurrence at/in both membranes. In this sense, electrochemical impedance spectroscopy may be used [24,63]. Another indication of the occurrence of sorption at/in the AEM is the behavior of the curves after the interruption of current application. Note that, differently from the cation-exchange membrane, the potential drop after current interruption (E_c – indicated in Fig. 5(a)) for the AEM dropped to a residual value very distant from zero. It is known that E_c appears due to differences in the concentration profiles established at both surfaces of the membrane during current application [29], thus, their values considerably far from zero for the AEM may be explained by the occurrence of intense SMX sorption at/in this membrane. The potential drop related to the diffusion relaxation of the membrane system did not approach zero over time, especially with the most concentrated solutions (0.01 g/L and 0.1 g/L). This behavior shown for the AEM curves confirms the suggestion made in Section 3.1.1 about the influence of H^+ ions on the desorption of SMX ions from the CEM. As the pH of the solutions used in the AEM evaluation was 9, they did not present a significant concentration of H^+ or OH^- ions, which could have desorbed the SMX ions.

Lastly, it was not possible to determine transition times for any solution used in the evaluations of the AEM, as the derivative curves did not show any peak related to this property (not shown herein). Therefore, the dependence of transition time on current density represented in Sand's coordinates could not be evaluated for the AEM. The impossibility of determining the transition time for the AEM can be explained by the extremely rapid occurrence of concentration polarization at this membrane, as already mentioned, due to almost instantaneous SMX sorption. According to the modified Sand equation [56], the reduction of the fraction of conductive area of the membrane, which can occur as a result of sorption, reduces the transition time.

3.2.2. Current-voltage curves for the AEM

The current–voltage curves constructed for the AEM with solutions at pH 9 and concentrations of 0.001 g/L, 0.005 g/L, 0.01 g/L and 0.1 g/L are present in Fig. 6, whereas the limiting current density and ohmic resistance values are present in Table 2. Unlike the curves presented for the CEM, the current–voltage curves of the AEM do not clearly show three well-defined regions, which hindered the determination of the limiting current density by the method described in Section 2.4 or by the well-known Cowan–Brown method [29]. Thus, the values of i_{lim} shown in Table 2 were estimated from the chronopotentiograms shown in Fig. 5 instead of the current–voltage curves. In this case, i_{lim} was considered as the current density at which the inflection point related to concentration polarization began to appear in the chronopotentiograms of each solution tested. The values of the anionic equivalent charge (Q_{eq}^-) of the solutions evaluated in this section are also present in Table 2, which were calculated similarly to the term Q_{eq}^+ of Eq. (2), but here only the anionic species present in the tested solution were considered.

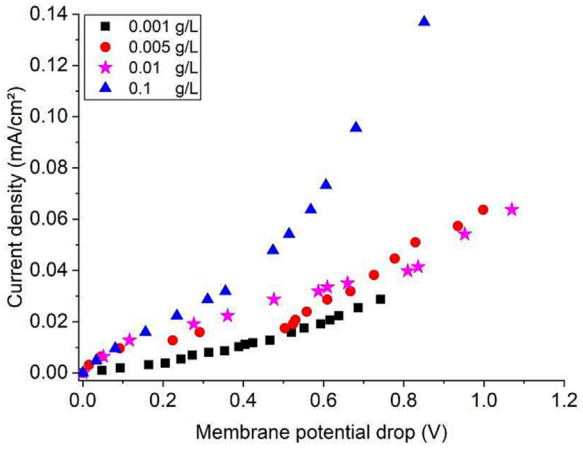

Fig. 6. Current-voltage curves for the anion-exchange membrane with SMX solutions at 0.001 g/L, 0.005 g/L, 0.01 g/L, and 0.1 g/L.

Table 2
Anionic equivalent charge (Q_{eq}^-), limiting current density (i_{lim}) and ohmic resistance (R_{ohm}) values obtained for the anion-exchange membrane with solutions at pH 9 and SMX concentrations of 0.001 g/L, 0.005 g/L, 0.01 g/L and 0.1 g/L.

SMX concentration (g/L)	0.001	0.005	0.01	0.1
Q_{eq}^-(meq/L)	4.0	19.8	39.5	394.5
i_{lim} (mA/cm^2)	0.007	0.014	0.019	0.026
R_{ohm} (Ω.cm^2)	51,391	7310	8082	10,025
Plateau length (V)	None	None	None	None

As shown in Fig. S4(b) of Supplementary Material, the limiting current densities obtained for the AEM show a linear relationship with the anionic equivalent charge only at concentrations between 0.001 g/L and 0.01 g/L since the value of i_{lim} for the 0.1 g/L solution is considerably lower than what was expected. This behavior was also verified for the CEM (Section 3.1.2), but with much greater intensity for the AEM, which supports the discussions on the greater intensity of sorption at/in the AEM than at/in the CEM. In this sense, the stronger reduction in the fraction of conductive area of the AEM as sorption occurred caused a greater reduction in its i_{lim}. The ohmic resistance decreased with increasing SMX concentration only from 0.001 g/L to 0.005 g/L. Note that from 0.005 g/L the increase in concentration caused the opposite effect. As verified for the CEM, this was due to the reduction of the area effectively available for ion exchange, as sorption causes membrane clogging. The plateau length for the AEM could not be determined because it was not possible to distinguish the three regions of the current–voltage curve.

4. Conclusions

A chronopotentiometric study was carried out to evaluate the transport of sulfamethoxazole at 0.001, 0.005, 0.01, and 0.1 g/L through a

cation- (pH 1.6) and anion–exchange membrane (pH 9) in the electrodialytic treatment of contaminated water and wastewater. Chronopotentiometry proved to be a valuable technique allowing to evaluate sorption phenomena occurrence at an ion-exchange membrane/aqueous solution interface.

The chronopotentiograms obtained for the CEM showed that electroconvection was the dominant overlimiting mechanism of ion transfer with the solution at 0.001 g/L. For the solution at 0.005 g/L, water dissociation was relevant and competitive with electroconvection. At higher concentrations (0.01 g/L and 0.1 g/L), electroconvection became negligible and the dominant overlimiting mechanisms was water dissociation. The initial (ohmic) potential drop and transition times values obtained from the curves indicated that the sorption phenomenon occurred at/in the CEM, especially with the most concentrated solutions. On the other hand, the potential drop profile during the relaxation of the membrane system showed that this phenomenon was reversible for the CEM under the conditions evaluated herein.

The chronopotentiograms obtained for the AEM with the most diluted solution (0.001 g/L) showed that the dominant overlimiting mechanism was water dissociation. The latter favored chemical equilibrium shifts at the membrane/solution interfaces, thus leading to the formation of neutral SMX species, which can impair the electrodialysis performance. The curves for the solution at 0.005 g/L showed that electroconvection and water dissociation occur simultaneously at this condition, whereas only electroconvection occurred intensely with the 0.01 g/L solution.

For all solutions tested, the profile of potential drop measured during and after application of current pulses showed that sorption occurs more strongly at/in the AEM than at/in the CEM. In the case of the AEM, sorption was an irreversible process, leading to the reduction of its conductive area. The current–voltage curves obtained for both membranes supported the findings inferred from the chronopotentiograms.

The greater intensity of sorption at/in the AEM than that at/in the CEM may be explained by the oppositely charged fixed functional groups of the membranes used and the different pH conditions of the solutions. Further work should be carried out using acidic and alkaline solutions presenting the same concentration of H^+ and OH^- ions, and target PhACs that are respectively negatively and positively charged under these two pH conditions.

CRediT authorship contribution statement

Kayo Santana Barros: Conceptualization, Data curation, Formal analysis, Investigation, Methodology, Validation, Visualization, Writing – original draft. **Alexandre Giacobbo:** Conceptualization, Investigation, Methodology, Visualization, Writing – review & editing. **Gustavo Dall Agnol:** Data curation. **Svetlozar Velizarov:** Writing – review & editing. **Valentín Pérez–Herranz:** Funding acquisition, Project administration, Supervision, Writing – review & editing. **Andréa Moura Bernardes:** Funding acquisition, Project administration, Resources, Supervision, Writing – review & editing.

Declaration of Competing Interest

The authors declare that they have no known competing financial interests or personal relationships that could have appeared to influence the work reported in this paper.

Acknowledgements

The authors gratefully acknowledge the financial support given by Ministerio de Universidades de España (European Union – Next Generation EU) and CNPq (grant numbers 408282/2018-5 and 117290/2021-1). This study was also financed by Grant RTI2018-101341-B-C21 funded by MCIN/AEI/10.13039/501100011033 and by "ERDF A way of making Europe".

Appendix A. Supplementary data

Supplementary data to this article can be found online at https://doi.org/10.1016/j.jelechem.2023.117214.

References

[1] N. Bolong, A.F. Ismail, M.R. Salim, T. Matsuura, A review of the effects of emerging contaminants in wastewater and options for their removal, Desalination. 239 (2009) 229–246, https://doi.org/10.1016/j.desal.2008.03.020.
[2] L. Goswami, R. Vinoth Kumar, S.N. Borah, N. Arul Manikandan, K. Pakshirajan, G. Pugazhenthi, Membrane bioreactor and integrated membrane bioreactor systems for micropollutant removal from wastewater: A review, J. Water Process Eng. 26 (2018) 314–328, https://doi.org/10.1016/j.jwpe.2018.10.024.
[3] A. Rodríguez-Rojas, J. Rodríguez-Beltrán, A. Couce, J. Blázquez, Antibiotics and antibiotic resistance: A bitter fight against evolution, Int. J. Med. Microbiol. 303 (2013) 293–297, https://doi.org/10.1016/j.ijmm.2013.02.004.
[4] A.R. Varela, O.C. Nunes, C.M. Manaia, Quinolone resistant Aeromonas spp. as carriers and potential tracers of acquired antibiotic resistance in hospital and municipal wastewater, Sci. Total Environ. 542 (2016) 665–671, https://doi.org/10.1016/j.scitotenv.2015.10.124.
[5] G. Prasannamedha, P.S. Kumar, A review on contamination and removal of sulfamethoxazole from aqueous solution using cleaner techniques: Present and future perspective, J. Clean. Prod. 250 (2020), https://doi.org/10.1016/j.jclepro.2019.119553 119553.
[6] S. Moradi, S.A. Sobhgol, F. Hayati, A.A. Isari, B. Kakavandi, P. Bashardoust, B. Anvaripour, Performance and reaction mechanism of MgO/ZnO/Graphene ternary nanocomposite in coupling with LED and ultrasound waves for the degradation of sulfamethoxazole and pharmaceutical wastewater, Sep. Purif. Technol. 251 (2020), https://doi.org/10.1016/j.seppur.2020.117373 117373.
[7] L. Shi, Z. Hu, Y. Wang, E. Bei, P.N.L. Lens, O. Thomas, Y. Hu, C. Chen, X. Zhan, In situ electrochemical oxidation in electrodialysis for antibiotics removal during nutrient recovery from pig manure digestate, Chem. Eng. J. 413 (2021), https://doi.org/10.1016/j.cej.2020.127485 127485.
[8] J.L. Acero, F.J. Benitez, F.J. Real, F. Teva, Micropollutants removal from retentates generated in ultrafiltration and nanofiltration treatments of municipal secondary effluents by means of coagulation, oxidation, and adsorption processes, Chem. Eng. J. 289 (2016) 48–58, https://doi.org/10.1016/j.cej.2015.12.082.
[9] A.R.D. Verliefde, S.G.J. Heijman, E.R. Cornelissen, G. Amy, B. Van der Bruggen, J. C. van Dijk, Influence of electrostatic interactions on the rejection with NF and assessment of the removal efficiency during NF/GAC treatment of pharmaceutically active compounds in surface water, Water Res. 41 (2007) 3227–3240, https://doi.org/10.1016/j.watres.2007.05.022.
[10] N. Nasrollahi, V. Vatanpour, A. Khataee, Removal of antibiotics from wastewaters by membrane technology: Limitations, successes, and future improvements, Sci. Total Environ. 838 (2022), https://doi.org/10.1016/j.scitotenv.2022.156010 156010.
[11] L. Shi, Z. Hu, W.S. Simplicio, S. Qiu, L. Xiao, B. Harhen, X. Zhan, Antibiotics in nutrient recovery from pig manure via electrodialysis reversal: Sorption and migration associated with membrane fouling, J. Memb. Sci. 597 (2020), https://doi.org/10.1016/j.memsci.2019.117633 117633.
[12] M. Roman, L. Gutierrez, L.H. Van Dijk, M. Vanoppen, J.W. Post, B.A. Wols, E.R. Cornelissen, A.R.D. Verliefde, Effect of pH on the transport and adsorption of organic micropollutants in ion-exchange membranes in electrodialysis-based desalination, Sep. Purif. Technol. 252 (2020), https://doi.org/10.1016/j.seppur.2020.117487 117487.
[13] M. Roman, L.H. Van Dijk, L. Gutierrez, M. Vanoppen, J.W. Post, B.A. Wols, E.R. Cornelissen, A.R.D. Verliefde, Key physicochemical characteristics governing organic micropollutant adsorption and transport in ion-exchange membranes during reverse electrodialysis, Desalination. 468 (2019), https://doi.org/10.1016/j.desal.2019.114084 114084.
[14] T. Scarazzato, K.S. Barros, T. Benvenuti, M.A. Siqueira Rodrigues, D.C. Romano Espinosa, A. Moura Bernardes, V. Pérez-Herranz, Achievements in electrodialysis processes for wastewater and water treatment, in: Curr. Trends Futur. Dev. Membr., Elsevier Inc., 2020, pp. 127–160, https://doi.org/10.1016/B978-0-12-817378-7.00005-7.
[15] T. Benvenuti, A. Giacobbo, C.D.M. da Trindade, K.S. Barros, T. Scarazzato. Electrodialysis, electrodialysis reversal and capacitive deionization technologies, in: Adv. Polym. Membr. Water Remediat., Elsevier Inc. 2022. 505–539. doi:10.1016/B978-0-323-88514-0.00014-0 505.
[16] K. Arola, A. Ward, M. Mänttäri, M. Kallioinen, D. Batstone, Transport of pharmaceuticals during electrodialysis treatment of wastewater, Water Res. 161 (2019) 496–504, https://doi.org/10.1016/j.watres.2019.06.031.
[17] E.H. Rotta, C.S. Bitencourt, L. Marder, A.M. Bernardes, Phosphorus recovery from low phosphate-containing solution by electrodialysis, J. Memb. Sci. 573 (2019) 293–300, https://doi.org/10.1016/j.memsci.2018.12.020.
[18] R.S. Kingsbury, F. Liu, S. Zhu, C. Boggs, M.D. Armstrong, D.F. Call, O. Coronell, Impact of natural organic matter and inorganic solutes on energy recovery from fi ve real salinity gradients using reverse electrodialysis, J. Memb. Sci. 541 (2017) 621–632, https://doi.org/10.1016/j.memsci.2017.07.038.

[19] M. Vanoppen, A.F.A.M. Bakelants, D. Gaublomme, K.V.K.M. Schoutteten, J. Van Den Bussche, L. Vanhaecke, A.R.D. Verliefde, Properties governing the transport of trace organic contaminants through ion-exchange membranes, Environ. Sci. Technol. 49 (2015) 489–497, https://doi.org/10.1021/es504389q.
[20] F.J. Borges, H. Roux-de Balmann, R. Guardani, Investigation of the mass transfer processes during the desalination of water containing phenol and sodium chloride by electrodialysis, J. Memb. Sci. 325 (2008) 130–138, https://doi.org/10.1016/j.memsci.2008.07.017.
[21] J.B. Welter, M.F. Simonaggio, S.W. da Silva, M.C. Martí-Calatayud, V. Pérez-Herranz, J.Z. Ferreira, Transport dynamics of atenolol in an electrodialysis cell: Membrane sorption and electric field-driven effects, J. Water Process Eng. 48 (2022), https://doi.org/10.1016/j.jwpe.2022.102870 102870.
[22] L. Ma, L. Gutierrez, T. Van Vooren, M. Vanoppen, M. Kazemabad, A. Verliefde, E. Cornelissen, Fate of organic micropollutants in reverse electrodialysis: Influence of membrane fouling and channel clogging, Desalination. 512 (2021), https://doi.org/10.1016/j.desal.2021.115114 115114.
[23] E.H. Rotta, M.C. Martí-Calatayud, V. Pérez-Herranz, A.M. Bernardes, Evaluation by Means of Electrochemical Impedance Spectroscopy of the Transport of Phosphate Ions through a Heterogeneous Anion-Exchange Membrane at Different pH and Electrolyte Concentration, Water. 15 (2022) 9, https://doi.org/10.3390/w15010009.
[24] M.C. Martí-Calatayud, E. Evdochenko, J. Bär, M. García-Gabaldón, M. Wessling, V. Pérez-Herranz, Tracking homogeneous reactions during electrodialysis of organic acids via EIS, J. Memb. Sci. 595 (2020), https://doi.org/10.1016/j.memsci.2019.117592 117592.
[25] A.A. Moya, E. Belashova, P. Sistat, Numerical simulation of linear sweep and large amplitude ac voltammetries of ion-exchange membrane systems, J. Memb. Sci. 474 (2015) 215–223, https://doi.org/10.1016/j.memsci.2014.10.006.
[26] A.A. Moya, P. Sistat, Reaching the limiting current regime by linear sweep voltammetry in ion-exchange membrane systems, J. Memb. Sci. 555 (2018) 134–145, https://doi.org/10.1016/j.memsci.2018.03.043.
[27] K.S. Barros, M.C. Martí-Calatayud, E.M. Ortega, V. Pérez-Herranz, D.C.R. Espinosa, Chronopotentiometric study on the simultaneous transport of EDTA ionic species and hydroxyl ions through an anion-exchange membrane for electrodialysis applications, J. Electroanal. Chem. 879 (2020), https://doi.org/10.1016/j.jelechem.2020.114782 114782.
[28] K.S. Barros, D.C.R. Espinosa, Chronopotentiometry of an anion-exchange membrane for treating a synthesized free-cyanide effluent from brass electrodeposition with EDTA as chelating agent, Sep. Purif. Technol. 201 (2018) 244–255, https://doi.org/10.1016/j.seppur.2018.03.013.
[29] K.S. Barros, M.C. Martí-Calatayud, T. Scarazzato, A.M. Bernardes, D.C.R. Espinosa, V. Pérez-Herranz, Investigation of ion-exchange membranes by means of chronopotentiometry: A comprehensive review on this highly informative and multipurpose technique, Adv. Colloid Interface Sci. 293 (2021), https://doi.org/10.1016/j.cis.2021.102439 102439.
[30] T. Scarazzato, Z. Panossian, M. García-Gabaldón, E.M. Ortega, J.A.S. Tenório, V. Pérez-Herranz, D.C.R. Espinosa, Evaluation of the transport properties of copper ions through a heterogeneous ion-exchange membrane in etidronic acid solutions by chronopotentiometry, J. Memb. Sci. 535 (2017) 268–278, https://doi.org/10.1016/j.memsci.2017.04.048.
[31] K.S. Barros, T. Scarazzato, V. Pérez-Herranz, D.C.R. Espinosa, Treatment of Cyanide-Free Wastewater from Brass Electrodeposition with EDTA by Electrodialysis: Evaluation of Underlimiting and Overlimiting Operations, Membranes (Basel). 10 (2020) 69, https://doi.org/10.3390/membranes10040069.
[32] D.I. de Souza, A. Giacobbo, E. da Silva Fernandes, M.A.S. Rodrigues, M.N. de Pinho, A.M. Bernardes, Experimental Design as a Tool for Optimizing and Predicting the Nanofiltration Performance by Treating Antibiotic-Containing Wastewater, Membranes (Basel) 10 (2020) 156, https://doi.org/10.3390/membranes10070156.
[33] D.G.J. Larsson, Pollution from drug manufacturing: review and perspectives, Philos. Trans. R. Soc. B Biol. Sci. 369 (2014) 20130571, https://doi.org/10.1098/rstb.2013.0571.
[34] G.C. Feijoo, K.S. Barros, T. Scarazzato, D.C.R. Espinosa, Electrodialysis for concentrating cobalt, chromium, manganese, and magnesium from a synthetic solution based on a nickel laterite processing route, Sep. Purif. Technol. 275 (2021), https://doi.org/10.1016/j.seppur.2021.119192 119192.
[35] K.S. Barros, A.L.V. Machado, V.S. Vielmo, S. Velizarov, J.Z. Ferreira, V. Pérez-Herranz, A.M. Bernardes, Membrane electrolysis for recovering Sb and Bi from elution solutions of ion-exchange resins used in copper electrorefining: A cyclic voltammetric study, J. Electroanal. Chem. 924 (2022), https://doi.org/10.1016/j.jelechem.2022.116867 116867.
[36] K.S. Barros, M.C. Martí-Calatayud, V. Pérez-Herranz, D.C.R. Espinosa, A three-stage chemical cleaning of ion-exchange membranes used in the treatment by electrodialysis of wastewaters generated in brass electroplating industries, Desalination. 492 (2020), https://doi.org/10.1016/j.desal.2020.114628 114628.
[37] ChemAxon, Chemicalize. (2019). https://chemicalize.com (accessed January 18, 2023).
[38] V.V. Nikonenko, A.V. Kovalenko, M.K. Urtenov, N.D. Pismenskaya, J. Han, P. Sistat, G. Pourcelly, Desalination at overlimiting currents: State-of-the-art and perspectives, Desalination. 342 (2014) 85–106, https://doi.org/10.1016/j.desal.2014.01.008.
[39] S. Mikhaylin, V. Nikonenko, N. Pismenskaya, G. Pourcelly, S. Choi, H.J. Kwon, J. Han, L. Bazinet, How physico-chemical and surface properties of cation-exchange membrane affect membrane scaling and electroconvective vortices: Influence on performance of electrodialysis with pulsed electric field, Desalination. 393 (2015) 102–114, https://doi.org/10.1016/j.desal.2015.09.011.
[40] R. Simons, Water splitting in ion exchange membranes, Electrochim. Acta. 30 (1985) 275–282, https://doi.org/10.1016/0013-4686(85)80184-5.
[41] R. Simons, Electric field effects on proton transfer between ionizable groups and water in ion exchange membranes, Electrochim. Acta. 29 (1984) 151–158, https://doi.org/10.1016/0013-4686(84)87040-1.
[42] M.C. Martí-Calatayud, M. García-Gabaldón, V. Pérez-Herranz, Effect of the equilibria of multivalent metal sulfates on the transport through cation-exchange membranes at different current regimes, J. Memb. Sci. 443 (2013) 181–192, https://doi.org/10.1016/j.memsci.2013.04.058.
[43] V.I. Zabolotsky, V.V. Nikonenko, N.D. Pismenskaya, On the role of gravitational convection in the transfer enhancement of salt ions in the course of dilute solution electrodialysis, J. Memb. Sci. 119 (1996) 171–181, https://doi.org/10.1016/0376-7388(96)00121-4.
[44] N. Pismenskaia, P. Sistat, P. Huguet, V. Nikonenko, G. Pourcelly, Chronopotentiometry applied to the study of ion transfer through anion exchange membranes, J. Memb. Sci. 228 (2004) 65–76, https://doi.org/10.1016/j.memsci.2003.09.012.
[45] N.D. Pismenskaya, V.V. Nikonenko, E.I. Belova, G.Y. Lopatkova, P. Sistat, G. Pourcelly, K. Larshe, Coupled convection of solution near the surface of ion-exchange membranes in intensive current regimes, Russ. J. Electrochem. 43 (2007) 307–327, https://doi.org/10.1134/S102319350703010X.
[46] L. Bazinet, T.R. Geoffroy, Electrodialytic Processes: Market Overview, Membrane Phenomena, Recent Developments and Sustainable Strategies, Membranes (Basel). 10 (2020) 221, https://doi.org/10.3390/membranes10090221.
[47] P. Sistat, G. Pourcelly, Chronopotentiometric response of an ion-exchange membrane in the underlimiting current-range. Transport phenomena within the diffusion layers, J. Memb. Sci. 123 (1997) 121–131, https://doi.org/10.1016/S0376-7388(96)00210-4.
[48] A.I. Schäfer, I. Akanyeti, A.J.C. Semião, Micropollutant sorption to membrane polymers: A review of mechanisms for estrogens, Adv. Colloid Interface Sci. 164 (2011) 100–117, https://doi.org/10.1016/j.cis.2010.09.006.
[49] W. Xue, F. Li, Q. Zhou, Bioresource Technology Degradation mechanisms of sulfamethoxazole and its induction of bacterial community changes and antibiotic resistance genes in a microbial fuel cell, Bioresour. Technol. 289 (2019), https://doi.org/10.1016/j.biortech.2019.121632 121632.
[50] S.C. Bisarya, D.M. Patil, Determination of salicylic-acid and phenol (ppm level) in effluent from aspirin plant, Res. Ind. 38 (1993) 170–172.
[51] L.J. Banasiak, B. Van der Bruggen, A.I. Schäfer, Sorption of pesticide endosulfan by electrodialysis membranes, Chem. Eng. J. 166 (2011) 233–239, https://doi.org/10.1016/j.cej.2010.10.066.
[52] S.A. Mareev, D.Y. Butylskii, N.D. Pismenskaya, V.V. Nikonenko, Chronopotentiometry of ion-exchange membranes in the overlimiting current range. Transition time for a finite-length diffusion layer: Modeling and experiment, J. Memb. Sci. 500 (2016) 171–179, https://doi.org/10.1016/j.memsci.2015.11.026.
[53] K.J. Vetter, Electrochemical kinetics: theoretical and experimental aspects., Acad. Press, New York, 1967.
[54] J.-H. Choi, S.-H. Moon, Pore size characterization of cation-exchange membranes by chronopotentiometry using homologous amine ions, J. Memb. Sci. 191 (2001) 225–236, https://doi.org/10.1016/S0376-7388(01)00513-0.
[55] M. García-Gabaldón, V. Pérez-Herranz, E. Ortega, Evaluation of two ion-exchange membranes for the transport of tin in the presence of hydrochloric acid, J. Memb. Sci. 371 (2011) 65–74, https://doi.org/10.1016/j.memsci.2011.01.015.
[56] K.S. Barros, T. Scarazzato, D.C.R. Espinosa, Evaluation of the effect of the solution concentration and membrane morphology on the transport properties of Cu(II) through two monopolar cation–exchange membranes, Sep. Purif. Technol. 193 (2018) 184–192, https://doi.org/10.1016/j.seppur.2017.10.067.
[57] W. Pronk, M. Biebow, M. Boller, Electrodialysis for recovering salts from a urine solution containing micropollutants, Environ. Sci. Technol. 40 (2006) 2414–2420, https://doi.org/10.1021/es051921i.
[58] N.D. Pismenskaya, V.V. Nikonenko, N.A. Melnik, K.A. Shevtsova, E.I. Belova, G. Pourcelly, D. Cot, L. Dammak, C. Larchet, Evolution with time of hydrophobicity and microrelief of a cation-exchange membrane surface and its impact on overlimiting mass transfer, J. Phys. Chem. B. 116 (2012) 2145–2161, https://doi.org/10.1021/jp2101896.
[59] M.A. Andreeva, V.V. Gil, N.D. Pismenskaya, L. Dammak, N.A. Kononenko, C. Larchet, D. Grande, V.V. Nikonenko, Mitigation of membrane scaling in electrodialysis by electroconvection enhancement, pH adjustment and pulsed electric field application, J. Memb. Sci. 549 (2018) 129–140, https://doi.org/10.1016/j.memsci.2017.12.005.
[60] J.H. Choi, S.H. Moon, Structural change of ion-exchange membrane surfaces under high electric fields and its effects on membrane properties, J. Colloid Interface Sci. 265 (2003) 93–100, https://doi.org/10.1016/S0021-9797(03)00136-X.
[61] K.S. Barros, E.M. Ortega, V. Pérez-Herranz, D.C.R. Espinosa, Evaluation of brass electrodeposition at RDE from cyanide-free bath using EDTA as a complexing agent, J. Electroanal. Chem. 865 (2020), https://doi.org/10.1016/j.jelechem.2020.114129 114129.
[62] V.V. Nikonenko, N.D. Pismenskaya, E.I. Belova, P. Sistat, P. Huguet, G. Pourcelly, C. Larchet, Intensive current transfer in membrane systems: Modelling, mechanisms and application in electrodialysis, Adv. Colloid Interface Sci. 160 (2010) 101–123, https://doi.org/10.1016/j.cis.2010.08.001.
[63] A.A. Moya, Electrochemical Impedance of Ion-Exchange Membranes with Interfacial Charge Transfer Resistances, J. Phys. Chem. C. 120 (2016) 6543–6552, https://doi.org/10.1021/acs.jpcc.5b12087.